Numerical Study of Propulsive Performance of Different Injection Patterns in Rotating Detonation Engine

Songbai Yao†, Yan Liu & Jianping Wang
College of Engineering, Peking University
Beijing 100871, China

1 Introduction

Rotating detonation engine (RDE) is one of the propulsion systems utilizing detonation waves for combustion, first performed by Voitsekhovskii [1] in 1960. Unlike traditional isobaric combustion, the detonation cycle has a close thermal efficiency to that of the isochoric cycle. Therefore, RDE is particularly attractive for aerospace propulsion and has been extensively studied [2–9]. Figure 1 shows a schematic of the annular combustion chamber of RDE.

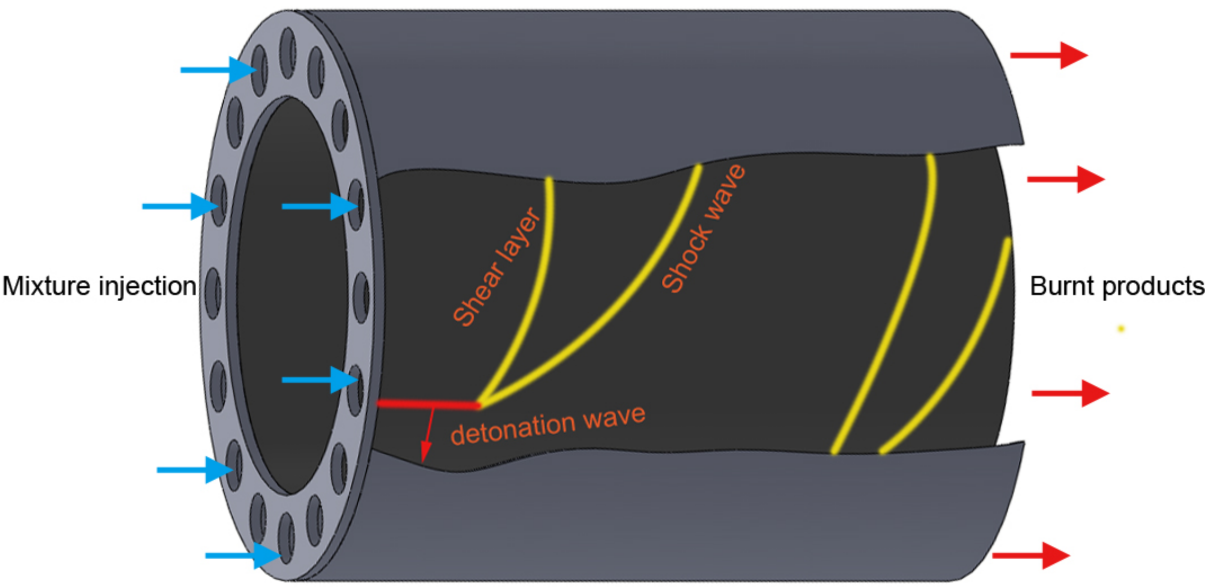

Figure 1: Schematic plot of RDE.

Liu et al. [10] propose four new different injection patterns in RDE, shown in Fig. 2, to improve the commonly used simple injection setting in numerical studies of RDE. In their simulations, the interaction between the detonation waves and combustion products caused by slits or intervals on the head wall of RDE combustor is discussed in detail. In the present study, the propulsive performances of RDE with these new injection patterns are numerically studied.

†Correspondence to: yaos@pku.edu.cn

2 Mathematical Formulations and Physical Configurations

Three-dimensional Euler equations with source term are used as governing equations, ignoring viscosity, thermal conduction and mass diffusion. The governing equations in generalized coordinates are

$$\frac{\partial \boldsymbol{U}}{\partial t}+\frac{\partial \boldsymbol{E}}{\partial \xi}+\frac{\partial \boldsymbol{F}}{\partial \eta}+\frac{\partial \boldsymbol{G}}{\partial \zeta}=\boldsymbol{S} \tag{1}$$

where the dependent variable vector $\boldsymbol{U}$, convective flux vectors $\boldsymbol{E}$, $\boldsymbol{F}$ and $\boldsymbol{G}$, and source vector $\boldsymbol{S}$ are defined as

$$\begin{gathered}
\boldsymbol{U}=[\rho\ \rho u\ \rho v\ \rho w\ e\ \rho\beta]^T, \\
\boldsymbol{E}=[\rho\bar{U}\ \rho\bar{U}u+p\xi_x\ \rho\bar{U}v+p\xi_y\ \rho\bar{U}w+p\xi_z\ \bar{U}(p+e)\ \rho\bar{U}\beta]^T, \\
\boldsymbol{F}=[\rho\bar{U}\ \rho\bar{U}u+p\xi_x\ \rho\bar{U}v+p\xi_y\ \rho\bar{U}w+p\xi_z\ \bar{U}(p+e)\ \rho\bar{U}\beta]^T, \\
\boldsymbol{G}=[\rho\bar{U}\ \rho\bar{U}u+p\xi_x\ \rho\bar{U}v+p\xi_y\ \rho\bar{U}w+p\xi_z\ \bar{U}(p+e)\ \rho\bar{U}\beta]^T, \\
\boldsymbol{S}=[0\ 0\ 0\ 0\ 0\ \rho w]^T.
\end{gathered}$$

The pressure p and temperature T are obtained through the equations of state

$$p=\rho(\gamma-1)[e-\beta_1 q-\frac{1}{2}\rho(u^2+v^2+w^2)] \tag{2}$$

and

$$T=\frac{p}{\rho R} \tag{3}$$

where $\bar{R}$ is the gas constant and γ is the heat ratio of the mixture, calculated as:

$$\bar{R}=\sum\beta_i\bar{R}_i \quad (i=1,2) \tag{4}$$

and

$$\gamma=\frac{\sum\beta_i\bar{R}_i\gamma_i/(\gamma_i-1)}{\sum\beta_i\bar{R}_i/(\gamma_i-1)} \quad (i=1,2) \tag{5}$$

where the subscript 1 and 2 refer to reactants and products, respectively. β_1 is the mass fraction of reactants while β_2 is that of products, $\beta_2=1-\beta_1$. The source term is treated as a stoichiometric hydrogen-air reaction using Arrhenius one-step chemistry model:

$$\dot{w}=\frac{d\beta_1}{dt}=-A\rho\beta_1 exp(-T_a/T) \tag{6}$$

where $\dot{w}$ is the mass production rate of reactants. The parameters of the one-step reaction model of hydrogen-air are adopted from the work of Ma et al. [11]. The average grid sizes in three dimensions are 0.8 mm. The flux terms are integrated by a fifth-order MPWENO scheme, and the third-order Runge-Kutta scheme is used for time integration.

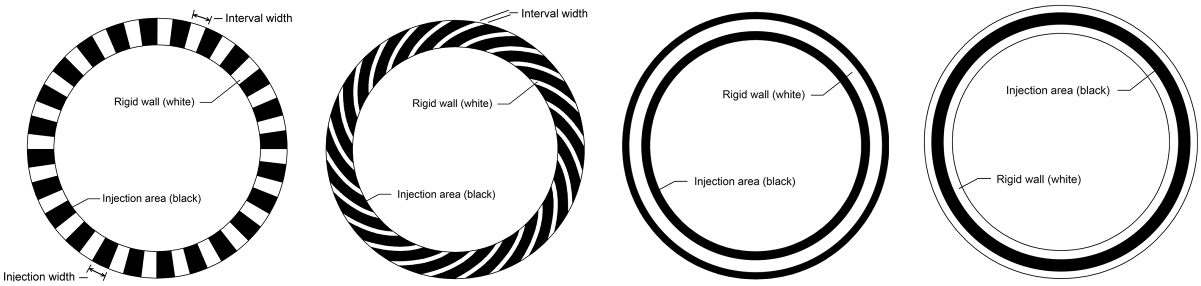

(a) Case1 (b) Case 2 (c) Case 3 (d) Case 4

Figure 2: Four new injection patterns [10].

3 Results and Discussion

In the present study, the propulsive performance of RDE are evaluated by the fuel-based specific impulse, defined as

$$I_{sp} = \frac{F}{\dot{m}_f g}. \tag{7}$$

where g is the acceleration of gravity and $\dot{m}_f$ is the mass flow rate of fuel. The fuel-based specific impulse of the above four cases are summarized in Table 1 with the standard case. It is found that the disparity is small among all these cases. This is probably because the specific impulse is related to the characteristics of the propellant, which is hydrogen-air mixture in the present model.

There are, however, significant difference in the fresh gas layers near the headwall of the combustor for case $1 \sim 4$. The characteristics of the injection patterns affect the fresh gas layers. Figure 3 shows the contour line of the fresh gas component of the standard case at 4000 μs. Compared with the standard case, the fresh gas layers are irregular and the height of the fresh gas wedges h are relatively smaller in case $1 \sim 4$, shown in Fig. 4. For case 1 and 2 with intervals in azimuthal direction, the fresh gas layers present wavy shape. Furthermore, the fresh gas layer in case 2 is more fragmented since its fuel injection is also discontinuous in radial direction. For case 3 and 4, h are a little higher than case 1 and 2. It is found that intervals in case 3 make the fresh gas layer more fragmented than that in case 4. Also, it can be seen that the shape of the fresh gas layer in case 4 is more like that of the standard case and case 4 has the highest h compared with other three cases.

The fresh gas layer plays an important role in self-sustaining detonation waves. The fresh gas layers in Fig. 4 show that there are more than one detonation waves. Therefore, the gaps between detonation waves should accumulate adequate fresh gas in front of the detonation wave fronts to sustain their propagation. To some extent, the irregularity and smaller h of the fresh gas layer in case $1 \sim 4$ reflect that the detonation wave fronts are relatively unstable compared with the standard case with full fuel injection. As a consequence, it is comparably difficult to initiate RDE and make it reach the stable state without full and uniform fuel injection. Thus, while the specific impulse of case $1 \sim 4$ does not show evident difference, the effects of the fuel injection pattern should be taken into consideration in experiments.

Table 1: Propulsive performance and characteristic parameters.

	Standard case	Case 1	Case 2	Case 3	Case 4
I_{sp} (s)	6527	6394	6505	6374	6465

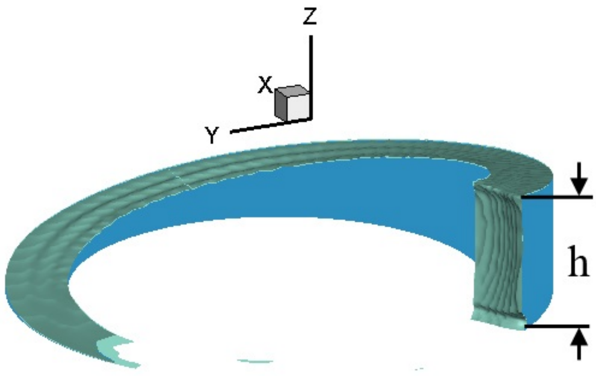

Figure 3: 3D fresh gas layer of the standard case.

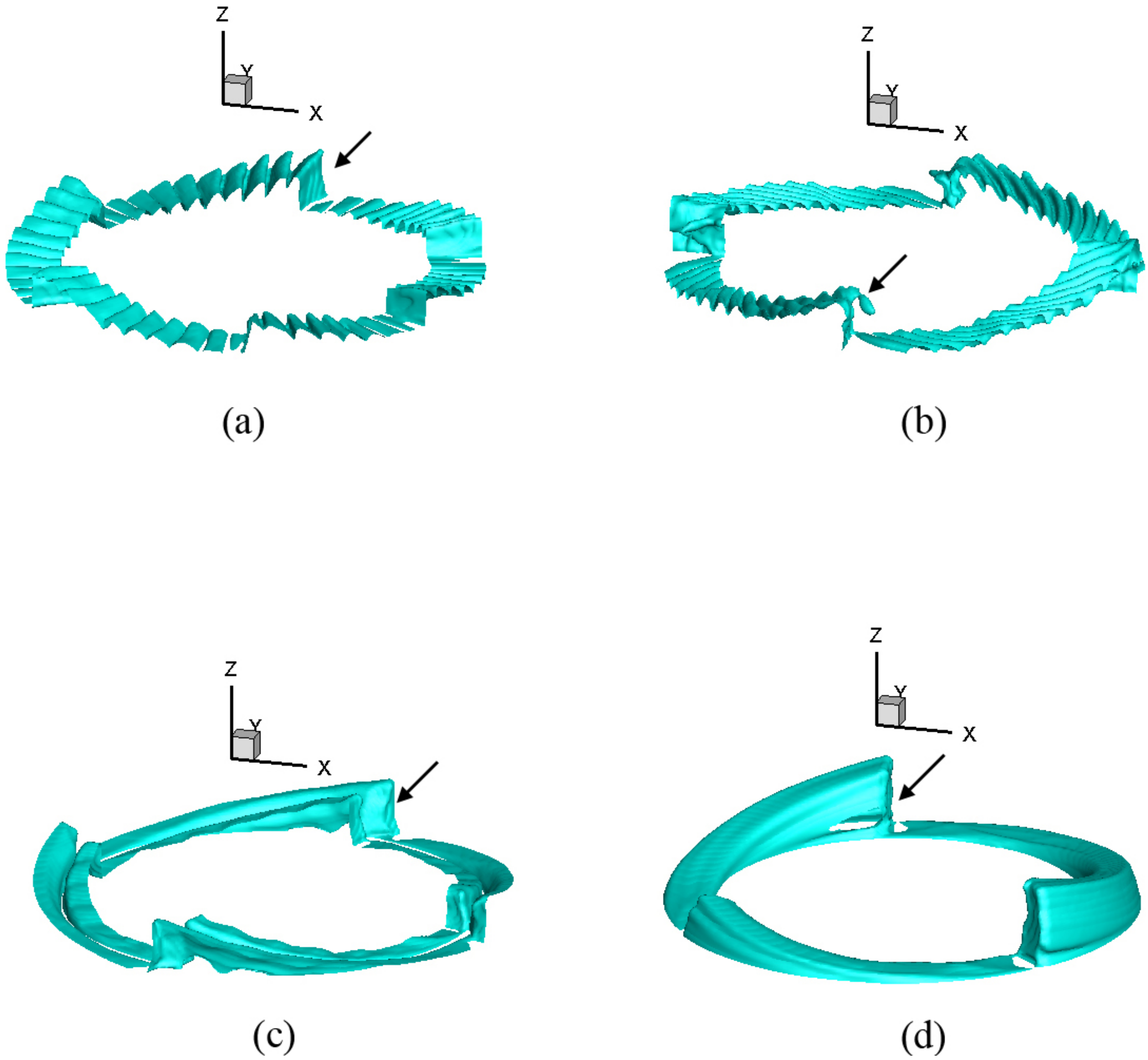

Figure 4: Isosurfaces of the fresh gas layer of case $1 \sim 4$.

4 Conclusions

The propulsive performance of four specific new injection patterns in RDE are discussed in the present study. Compared with the commonly used simple full injection setting, those new injection patterns are more accordant with actual conditions in experimental researches on RDE and practical applications for the reason that the fuel injection can be nonuniform. Our simulations show that the specific impulse is not distinctly affected by the fuel injection on the head wall of the chamber. In this respect, the effects of fuel injection patterns on the propulsive performance of RDE are not apparent. However, these new injection patterns bring in significant difference in the fresh gas layers. Discontinuous fuel injection in radial and azimuthal direction make the fresh gas layers irregular and the height of the fresh gas wedges h become smaller. These two aspects have influence on the stability of detonation waves.

References

[1] Voitsekhovskii (1959). Stationary Spin Detonation. Dokl. Akad. Nauk SSSR Vol. 3, No. 6 pp. 157-164.

[2] Bykovskii, F. A., Zhdan, S. A., and Vedernikov, E. F. (2006). Continuous Spin Detonation. J. Propuls. Power Vol. 22, No. 6 pp. 1204-1216.

[3] Kindracki, J., Wolanski, P., and Gut, Z. (2011). Experimental Research on the Rotating Detonation in Gaseous Fuels-Oxygen Mixture. Shock Waves Vol. 21, No. 2 pp. 75-87.

[4] Fujiwara, T., Hishida, M., and Wolanski, P. (2009). Stabilization of Detonation for Any Incoming Mach Numbers. Combust. Expl. Shock Waves Vol. 45, No. 5 pp. 603-605.

[5] Davidenko, D. M., Gokalp, I., and Kudryavtsev, A. N. (2008). Numerical Study of the Continuous Detonation Wave Rocket Engine.AIAA paper 2008-2680.

[6] Yi, T. H., Lou, J., Turangan, C., Choi, J. Y., and Wolanski, P. (2011). Propulsive Performance of a Continuously Rotating Detonation Engine.J. Propuls. Power Vol. 27, No. 1 pp. 171-181.

[7] Schwer, D., and Kailasanath, K. (2013). Fluid Dynamics of Rotating Detonation Engines with Hydrogen and Hydrocarbon Fuels.Combust. Inst. Vol. 34, No. 2 pp. 1991-1998.

[8] Tang, X. M., Wang, J. P., and Shao, Y. T. (2015). Three-dimensional Numerical Investigation of the Rotating Detonation Engine with a Hollow Combustor.Combust. Flame Vol. 162, No. 4 pp. 997-1008.

[9] Liu, S. J., Lin, Z. Y., Liu, W. D., Liu, W., and Zhuang, F. C. (2012). Experimental Realization of H_2/Air Continuous Rotating Detonation in a Cylindrical Combustor.Combust. Sci. Technol. Vol. 184, No. 9 pp. 1302-1317.

[10] Liu, M, Zhou, R., and Wang, J. P. (2015). Numerical Investigation of Different Injection Patterns in Rotating Detonation Engines. Combust. Sci. Technol. Vol. 187, No. 3 pp. 343-361.

[11] Ma, F., Choi, J. Y., and Yang, V. (2006) Propulsive Performance of Airbreathing Pulse Detonation Engines. J. Propuls. Power Vol. 22, No. 6, pp. 1188-1203.